Title:	Simulation of Stator Winding Faults with an Analytical Model of a PMSM
Authors:	Simon Foitzik, Martin Doppelbauer
Institute:	Karlsruhe Institute of Technology (KIT) Institute of Electrical Engineering (ETI)
Type:	Conference Proceedings
Published at:	2018 IEEE International Conference on Power Electronics, Drives and Energy Systems (PEDES) Publisher: IEEE Year: 2019 ISBN: 978-1-5386-9315-5 Pages: 1-6
Hyperlinks:	https://ieeexplore.ieee.org/document/8707719

Simulation of Stator Winding Faults with an Analytical Model of a PMSM

Simon Foitzik
Institute of Electrical Engineering (ETI)
Karlsruhe Institute of Technology (KIT)
Karlsruhe, Germany
simon.foitzik@kit.edu

Martin Doppelbauer
Institute of Electrical Engineering (ETI)
Karlsruhe Institute of Technology (KIT)
Karlsruhe, Germany
martin.doppelbauer@kit.edu

Abstract—Stator winding faults are one of the major limitations of the lifetime and reliability of electrical machines. Inter-turn faults are for that matter often the origin of more severe faults, which can lead to complete system failures. This paper presents an analytical machine model, to investigate the behavior of PMSMs with dynamic stator winding faults on turn level. In order to keep the model compact, the levels of abstraction can be adapted within the machine model. The acausal implementation of the electric domain allows the simulation of one model with different operating modes. This paper compares the simulation results of the analytical model with FEA simulation results. The average torque differs in case of two inter-turn faults at nominal load operation by 2 % and the amplitude of the fault currents differs by 5 %. There is no difference in the frequencies and phase angles of the fault currents and the torque. In our future work, we will use the presented model to develop a fault management system, allowing fault tolerant operation of safety critical applications.

Index Terms—stator winding faults, inter-turn faults, PMSM, buried magnets, acausal implementation, analytical model

I. Introduction

Fault tolerant propulsion systems are gaining a lot of attention in recent years. One reason is their inevitable use for upcoming topics in safety critical applications like all electric aircraft [1]. In this context, the term fault tolerant means that the propulsion system can still operate with full or reduced power, when a fault occurs. To enable a fault tolerant operation, a fault management system must be installed [2]. This system contains detailed knowledge of the complete propulsion system under healthy and faulty conditions. Initial faults in the stator winding of electrical machines are mainly inter-turn faults [3]. It is essential for the fault management system to detect these minor faults in an early stage and react with countermeasures [4]. Otherwise, the inter-turn fault propagates to more serious faults, such as a phase-to-phase or a phase-to-ground short circuit. These secondary order faults can have severe impacts in safety critical applications and can lead to complete system failures. The accurate modeling of inter-turn faults in the stator winding is therefore of high interest.

Several methods of analytical inter-turn fault modeling already exist [5]–[7]. In these papers, they assume permanent magnet synchronous machines (PMSMs) with surface mounted magnets on the rotor, which means that the phase inductance is independent of the rotor position. Furthermore,

they limit the number of stator winding faults to a single inter-turn fault. It is unlikely that this limitation stays true for an actual fault in the stator winding. The simulation of a complete fault network is therefore not feasible, which restricts the accuracy of the fault analysis.

This paper presents a new approach to simulate an analytical model of a PMSM with different inductance in d- and q-axis. We propose to define the magnetic coupling on turn level for the faulty part of the stator winding. The electric circuit of the model is acausal implemented, which allows the simulation with either a current or a voltage source. This approach allows the analysis of advanced stator winding fault scenarios and offers therefore a more detailed analysis compared to existing approaches.

II. Modeling

Inter-turn faults occur most likely at the first turns of a coil, due to increased voltage stress in adjustable-speed drive systems [8]. The machine must be modeled on turn level in the faulty machine part, to enable inter-turn fault simulation. The healthy machine part can be summarized to a more abstract level, which allows a compact model. Thus, the machine model contains different levels of abstraction, depending on the investigated fault scenario. The different levels include the turn (T) level, coil (C) level and phase (Ph) level, as it is shown in Fig. 1. The phase inductance is separated into the phase inductance per pole P1 and P2. In this paper, we want to analyze stator winding faults in phase Ph1. If we want to analyze for example inter-turn faults between two different phases, the second involved phase must also be modeled on
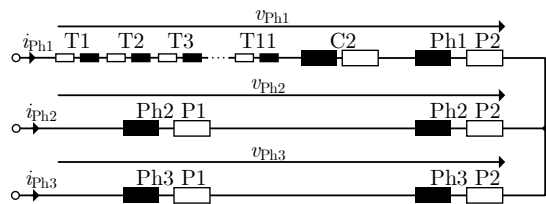

Fig. 1. Implemented electric circuit of the machine model.

turn level. The stator winding configuration must be known, to develop an analytical model on turn level.

A. Assumptions

We use the following assumptions to model the PMSM. We assume three distributed, symmetric, full-pitched and star-connected phases of the stator winding and the neutral point of the machine is not attached to the converter. The stator winding parameters of the analyzed machine are summarized in Table I. The magnetic circuit is linear and the permeability of the iron approaches infinity. There is no magnetic coupling among different pole pairs. Only the fundamental wave is regarded. The stator winding end effects are neglected. Friction loss, iron loss, dielectric currents, skin effects and proximity effects are neglected. The physical geometry is transformed into a model with a constant air-gap length. The centers of the slots define a threadlike surface current. We assume that the flux linkage Ψ_{PM} and the inductance L_{d} and L_{q} are given. These values are obtained by either theoretical calculation, Finite Element Analysis (FEA) simulation or the data sheet of a machine.

B. Voltage and Flux Linkage Equations

The voltage equation for all turns, coils and phases in matrix notation can be derived [9]:

$$v_x = R_x i_x + \frac{\mathrm{d}}{\mathrm{d}t} \Psi_x \qquad (1)$$

Therein v_x denotes the vector of the voltages, R_x the matrix of the ohmic resistance, i_x the vector of the currents and Ψ_x the vector of the flux linkages with $x \in \{\mathrm{T}, \mathrm{C}, \mathrm{Ph}\}$. The time is denoted by t. The flux linkage vectors are calculated:

$$\Psi_{\mathrm{T}} = L_{\mathrm{T,T}} i_{\mathrm{T}} + L_{\mathrm{T,C}} i_{\mathrm{C}} + L_{\mathrm{T,Ph}} i_{\mathrm{Ph}} + \Psi_{\mathrm{T,PM}} \qquad (2)$$

$$\Psi_{\mathrm{C}} = L_{\mathrm{C,T}} i_{\mathrm{T}} + L_{\mathrm{C,C}} i_{\mathrm{C}} + L_{\mathrm{C,Ph}} i_{\mathrm{Ph}} + \Psi_{\mathrm{C,PM}} \qquad (3)$$

$$\Psi_{\mathrm{Ph}} = L_{\mathrm{Ph,T}} i_{\mathrm{T}} + L_{\mathrm{Ph,C}} i_{\mathrm{C}} + L_{\mathrm{Ph,Ph}} i_{\mathrm{Ph}} + \Psi_{\mathrm{Ph,PM}} \qquad (4)$$

Therein the matrix $L_{x,y}$ marks the inductive coupling from element y to element x, with $x, y \in \{\mathrm{T}, \mathrm{C}, \mathrm{Ph}\}$. For example the matrix $L_{\mathrm{T,T}}$ (11×11) describes the inductive coupling among the turns T1...T11, the matrix $L_{\mathrm{T,C}}$ (11×1) describes the inductive coupling from the coil C2 to the turns and the matrix $L_{\mathrm{T,Ph}}$ (11×5) describes the inductive coupling from the phases per pole to the turns. The vector $\Psi_{x,\mathrm{PM}}$ denotes the flux linkage in element x, which results from the permanent magnets of the rotor. For example the vector $\Psi_{\mathrm{T,PM}}$ (11×1)

denotes the permanent magnet flux linkage of the turns from coil C1. The permanent magnet flux linkage depends on the rotor position and the rotor angle must therefore be defined for each inductance. In Fig. 2 the rotor angles γ, γ_{C1} and γ_{C2} are shown. The colored circles and crosses in the slots define a positive and negative current flow direction, to determine the direction of magnetization and thus the axis of each inductance. The rotor angle γ is defined as the angle between the d-axis and the α-axis of the stator. The d-axis is defined by the magnetic flux of the magnets in the rotor and the α-axis equals the Ph1-axis. The rotor angles $\gamma_{\mathrm{C1}} = \gamma + \frac{2\pi}{2 \cdot N}$ and $\gamma_{\mathrm{C2}} = \gamma - \frac{2\pi}{2 \cdot N}$ can be calculated by γ and the number of slots N. The permanent magnet flux linkage of the turns, coils and phases is calculated by:

$$\Psi_{\mathrm{T1...T11,PM}} = \frac{\Psi_{\mathrm{PM}}}{p \cdot q \cdot \xi \cdot w_{\mathrm{C}}} \cdot \cos(\gamma_{\mathrm{C1}}) \qquad (5)$$

$$\Psi_{\mathrm{C2}} = \frac{\Psi_{\mathrm{PM}}}{p \cdot q \cdot \xi} \cdot \cos(\gamma_{\mathrm{C2}}) \qquad (6)$$

$$\Psi_{\mathrm{Ph1\,P1,PM}} = \Psi_{\mathrm{Ph1\,P2,PM}} = \frac{\Psi_{\mathrm{PM}}}{p} \cdot \cos(\gamma) \qquad (7)$$

$$\Psi_{\mathrm{Ph2\,P1,PM}} = \Psi_{\mathrm{Ph2\,P2,PM}} = \frac{\Psi_{\mathrm{PM}}}{p} \cdot \cos(\gamma - \frac{2\pi}{3}) \qquad (8)$$

$$\Psi_{\mathrm{Ph3\,P1,PM}} = \Psi_{\mathrm{Ph3\,P2,PM}} = \frac{\Psi_{\mathrm{PM}}}{p} \cdot \cos(\gamma - \frac{4\pi}{3}) \qquad (9)$$

Therein p denotes the number of pole pairs, q the number of slots per pole and phase, w_{C} the number of turns per coil, m the number of phases and ξ the winding factor, which is calculated by:

$$\xi = \frac{\sin\left(\frac{\pi}{2 \cdot m}\right)}{q \cdot \sin\left(\frac{\pi}{2 \cdot m \cdot q}\right)} \qquad (10)$$

C. Inductance Equation

The calculation of the turn, coil and phase per pole inductance is derived by the voltage equation of the electric circuit. The voltage of phase Ph1 is according to Fig. 1 calculated by:

$$v_{\mathrm{Ph1}} = \sum_{j=1}^{11} v_{\mathrm{T}j} + v_{\mathrm{C2}} + v_{\mathrm{Ph1P2}} \qquad (11)$$

TABLE I
STATOR WINDING PARAMETERS

parameters	values
number of phases	3
number of pole pairs	2
number of slots per pole per phase	2
number of parallel paths	1
number of parallel turns	1
number of turns per coil	11
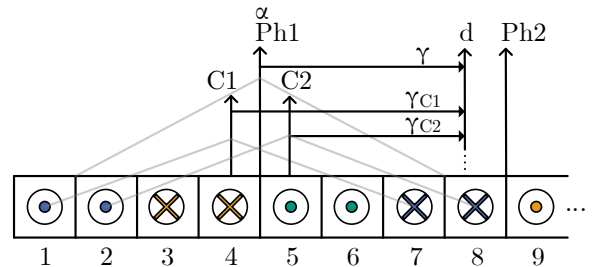
Fig. 2. Simplified stator representation with the definition of the rotor angles γ, γ_{C1} and γ_{C2}.

The voltages $v_{T1...11}$, v_{C2} and v_{Ph1P2} are calculated by (1)-(4) and the voltage v_{Ph1} for a phase model is calculated by [9]:

$$v_{Ph1} = R_{Ph1} \cdot i_{Ph1} + \frac{d}{dt} \big(L_{Ph1,Ph1} \cdot i_{Ph1} \tag{12}$$
$$+ L_{Ph1,Ph2} \cdot i_{Ph2} + L_{Ph1,Ph3} \cdot i_{Ph3} + \Psi_{PM} \cdot \cos(\gamma) \big)$$

Equation (11) and (12) show the linkage between the phase inductance and the elements of phase Ph1 of Fig. 1. This means we can calculate the individual inductance based on the voltage equation of the electric circuit and the phase inductance. For a healthy machine with a magnetic circuit depending on the rotor position, we can describe the phase inductance by the two parts L_{S0} and L_{S2} [9]:

$$L_{S0} = \frac{1}{3} \cdot (L_d + L_q) \tag{13}$$

$$L_{S2} = \frac{1}{3} \cdot (L_d - L_q) \tag{14}$$

With this information, we can calculate the phase inductance:

$$L_{Ph1,Ph1} = L_{S0} + L_{S2} \cdot \cos(2\gamma) \tag{15}$$

$$L_{Ph2,Ph2} = L_{S0} + L_{S2} \cdot \cos(2\gamma - \frac{4\pi}{3}) \tag{16}$$

$$L_{Ph3,Ph3} = L_{S0} + L_{S2} \cdot \cos(2\gamma - \frac{2\pi}{3}) \tag{17}$$

$$L_{Ph1,Ph2} = L_{Ph2,Ph1} = -\frac{1}{2}L_{S0} + L_{S2} \cdot \cos(2\gamma - \frac{2\pi}{3}) \tag{18}$$

$$L_{Ph1,Ph3} = L_{Ph3,Ph1} = -\frac{1}{2}L_{S0} + L_{S2} \cdot \cos(2\gamma - \frac{4\pi}{3}) \tag{19}$$

$$L_{Ph2,Ph3} = L_{Ph3,Ph2} = -\frac{1}{2}L_{S0} + L_{S2} \cdot \cos(2\gamma) \tag{20}$$

The resulting equations for the turn, coil and phase inductance are shown in Table II.

D. Power Equation

The power equation is derived by multiplying the voltage equation (1) with the transposed current vector $\boldsymbol{i}_x^T$ [9]:

$$\boldsymbol{i}_x^T \boldsymbol{v}_x = \boldsymbol{i}_x^T \boldsymbol{R}_x \boldsymbol{i}_x + \boldsymbol{i}_x^T \frac{d}{dt} \boldsymbol{\Psi}_x \tag{21}$$

$$P_{el} = P_{loss} + \frac{dW_{mag}}{dt} + P_{i,mech} \tag{22}$$

The electric power P_{el} separates into the power loss P_{loss}, the derivative of the stored magnetic energy $\frac{dW_{mag}}{dt}$ and the inner mechanical power $P_{i,mech}$. The power loss equals the resistive loss and this means:

$$\frac{dW_{mag}}{dt} + P_{i,mech} = \boldsymbol{i}_x^T \frac{d}{dt} \boldsymbol{\Psi}_x \tag{23}$$

In a machine with a symmetric matrix of the phase inductance, the average of the term $\frac{dW_{mag}}{dt}$ is zero over time and can be neglected. The equation for the electromagnetic torque T_{el} can be derived, wherein Ω denotes the angular velocity of the rotor:

$$T_{el} \cdot \Omega = \boldsymbol{i}_x^T \frac{d}{dt} \boldsymbol{\Psi}_x \tag{24}$$

$$= \sum_j i_{Tj} \frac{d}{dt} \Psi_{Tj} + \sum_k i_{Ck} \frac{d}{dt} \Psi_{Ck} \tag{25}$$

$$+ \sum_l i_{Phl} \frac{d}{dt} \Psi_{Phl}$$

III. Implementation

The aim of the developed model is to investigate the machine behavior under various stator winding fault scenarios. The machine behavior is not only dependent on the machine itself, but also on the operating mode. We can use either a current source or a current controlled voltage source, to set a desired torque according to (24). The use of both power sources is essential for the analysis of the machine and denotes two different operating modes. With the current source, we can analyze the pure machine behavior without interference of a controller. Adjustable-speed drive systems use current controlled voltage source inverters. Therefore, it is necessary for practical applications, to be able to simulate the same machine model with a voltage source and analyze the interference with the current controller.

A. Causal Implementation

Machine models are often implemented with a predefined information flow direction and can only be simulated with a voltage source [10], [11]. This way of implementation is also called causal implementation. The disadvantage of such

TABLE II
MACHINE INDUCTANCE

	T1...T11	C2	Ph2 P1	Ph3 P1	Ph1 P2	Ph2 P2	Ph3 P2
T1...T11	$\frac{L_{Ph1,Ph1}}{p \cdot (q \cdot w_C)^2}$	$\frac{L_{Ph1,Ph1}}{p \cdot q^2 \cdot w_C}$	$\frac{L_{Ph1,Ph2}}{p \cdot q \cdot w_C}$	$\frac{L_{Ph1,Ph3}}{p \cdot q \cdot w_C}$	-	-	-
C2	$\frac{L_{Ph1,Ph1}}{p \cdot q^2 \cdot w_C}$	$\frac{L_{Ph1,Ph1}}{p \cdot q^2}$	$\frac{L_{Ph1,Ph2}}{p \cdot q}$	$\frac{L_{Ph1,Ph3}}{p \cdot q}$	-	-	-
Ph2 P1	$\frac{L_{Ph2,Ph1}}{p \cdot q \cdot w_C}$	$\frac{L_{Ph2,Ph1}}{p \cdot q}$	$\frac{L_{Ph2,Ph2}}{p}$	$\frac{L_{Ph2,Ph3}}{p}$	-	-	-
Ph3 P1	$\frac{L_{Ph3,Ph1}}{p \cdot q \cdot w_C}$	$\frac{L_{Ph3,Ph1}}{p \cdot q}$	$\frac{L_{Ph3,Ph2}}{p}$	$\frac{L_{Ph3,Ph3}}{p}$	-	-	-
Ph1 P2	-	-	-	-	$\frac{L_{Ph1,Ph1}}{p}$	$\frac{L_{Ph1,Ph2}}{p}$	$\frac{L_{Ph1,Ph3}}{p}$
Ph2 P2	-	-	-	-	$\frac{L_{Ph2,Ph1}}{p}$	$\frac{L_{Ph2,Ph2}}{p}$	$\frac{L_{Ph2,Ph3}}{p}$
Ph3 P2	-	-	-	-	$\frac{L_{Ph3,Ph1}}{p}$	$\frac{L_{Ph3,Ph2}}{p}$	$\frac{L_{Ph3,Ph3}}{p}$

an implementation is the fixed specification of the input and output ports of the system. Thus, the simulation with varying operating modes is not possible.

B. Acausal Implementation

We use an acausal implementation with a nondirectional information flow [12], to eliminate the disadvantages of the causal implementation. Generalized variables are used to calculate the energy transfer among the physical domains. The behavior of the electrical domain is described by differential equations. The solution of the differential equations depends on the given boundary conditions. This means that the input and output ports of the machine model do not need to be preliminary defined. They are defined during the model compilation at the beginning of the simulation, subject to the operating mode. Therefore, we can use either a current source, a voltage source or no electric power source, to operate the machine. The analytical model of the PMSM is implemented in MATLAB® Simscape™. Each turn, coil and phase of the electric domain is modeled by a customized component, which includes the corresponding voltage equation (1). The proposed implementation is shown in Fig. 3. The flux linkage is calculated online by the equations (2), (3) and (4) during the simulation. The connection of all customized components forms the stator winding of the machine. Fig. 1 shows the resulting electric circuit of the analyzed PMSM. For the analysis of a stator winding fault, the electric circuit can be extended by passive components. With the resulting fault network, we can simulate for example inter-turn faults, phase-to-phase faults or phase-to-ground faults. In contrast to the FEA simulation, this implementation allows a simulation with variable angular velocity and time-variant fault components. Furthermore, the computation time of the analytical model is about 200 times faster.

IV. FINITE ELEMENT ANALYSIS

We use a 2D FEA in this paper to compare the simulation results of the analytical model. The FEA simulation is performed with the software Flux-2D from Altair and considers the nonlinear magnetic circuit. Fig. 4 shows the cross section of the analyzed PMSM with buried magnets. The electric circuit of the FEA model equals the electric circuit of the analytical model. It is essential to take the complete cross section of the PMSM for the FEA model into account, without utilizing any periodicity. Otherwise, the stator winding faults
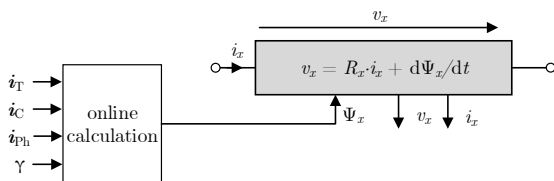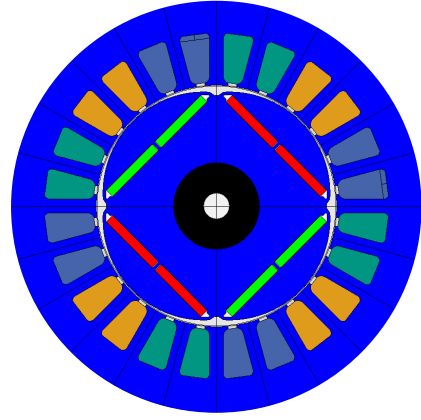

Fig. 4. Cross section of the analyzed PMSM with buried magnets.

would also be repeated periodically. The FEA model is also used to determine the flux linkage Ψ_{PM} and the inductance L_{d} and L_{q}, by linearization at the nominal operating point. The machine parameters are summarized in Table III.

V. RESULTS

The simulation results of the analytical and FEA model are presented and compared under healthy and faulty conditions for the no-load and the nominal load operation. Both models use a current source to set the nominal load operation and to achieve comparable results. The Maximum Torque per Ampere (MTPA) approach defines the phase currents for the nominal load operation. For the presented PMSM the nominal MTPA point equals $i_{\mathrm{q}} = 8.4\,\mathrm{A}$ and $i_{\mathrm{d}} = $ -1.5 A at 3000 rpm and 2.5 Nm.

A. Healthy Machine

Fig. 5 shows the simulation results for the healthy machine for the nominal operating point. The FEA simulation shows that the amplitude of the torque ripple is 0.2 Nm. The analytical model only regards the fundamental wave and therefore the torque is constant.

B. Faulty Machine

As already explained, inter-turn faults occur most likely at the first turns of a coil. We assume two inter-turn faults in

Fig. 3. Customized component of an inductance.

TABLE III
MACHINE PARAMETERS

parameters	values
ohmic stator resistance	55.6 mΩ
inductance in d-axis	0.67 mH
inductance in q-axis	1.9 mH
permanent magnet flux linkage	98 mVs
nominal voltage	32 V
nominal current	8.5 A
nominal speed	3000 rpm
nominal torque	2.5 Nm
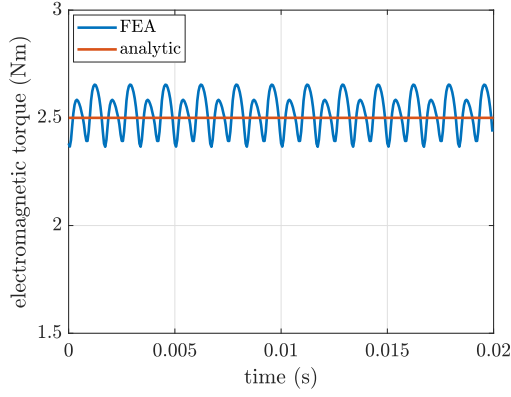
Fig. 5. Simulation results of the healthy machine. A current source with $i_\mathrm{q} = 8.4\,\mathrm{A}$ and $i_\mathrm{d} = -1.5\,\mathrm{A}$ is used for the power supply and the rotor speed is $3000\,\mathrm{rpm}$.

coil C1, which is shown in Fig. 6. The short circuit paths are marked red, which represents the damaged isolation at these points. The isolation between the coil and the stator is marked green and the encapsulating resin is pastel-colored. We include the fault resistors R_F1 and R_F2 to the electric circuit of the stator winding, to take the stator winding faults into account. The extended circuit is shown in Fig. 7. The fault network is identical for the analytical and the FEA model. The fault resistors R_F1 and R_F2 are time-variant for the analytical model. This behavior emulates the propagation of the inter-turn faults, caused by the accruing thermal stress. At $t = 0\,\mathrm{s}$ the fault resistors are constant $R_\mathrm{F1} = R_\mathrm{F2} = 1\mathrm{k}\,\Omega$. After $5\,\mathrm{ms}$ the fault resistors start to decrease exponentially to a final value of $R_\mathrm{F1} = R_\mathrm{F2} = 100\,\mathrm{m}\Omega$ for the no-load operation and to a final value of $R_\mathrm{F1} = R_\mathrm{F2} = 50\,\mathrm{m}\Omega$
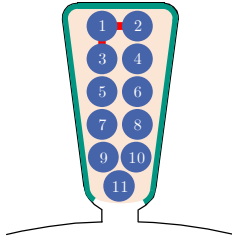

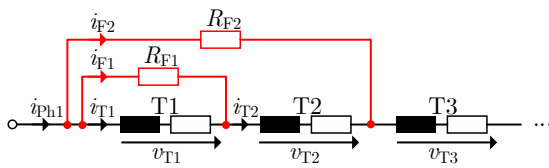Fig. 6. Slot with one coil side of C1, including two red marked inter-turn faults.

Fig. 7. Implemented electric circuit of the analyzed PMSM with two inter-turn faults in phase Ph1.
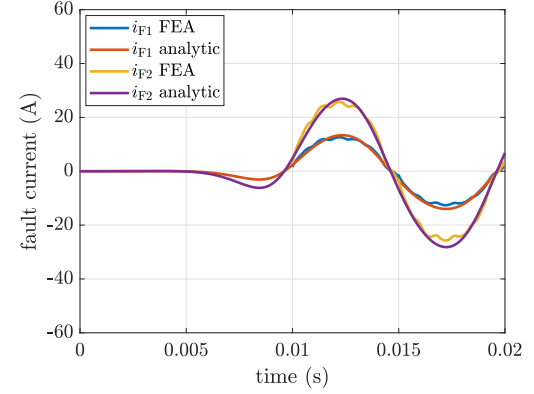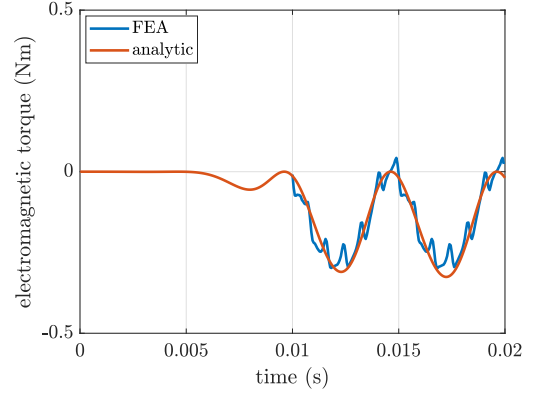

Fig. 8. Simulation results of the analyzed fault network in coil C1 of the stator winding. The machine is in no-load operation and the rotor speed is $3000\,\mathrm{rpm}$.

for the nominal load operation. The time constant of the exponential function is $\tau = 1\,\mathrm{ms}$. The fault resistors are in the FEA simulation constant $R_\mathrm{F1} = R_\mathrm{F2} = 100\,\mathrm{m}\Omega$ and $R_\mathrm{F1} = R_\mathrm{F2} = 50\,\mathrm{m}\Omega$, respectively. Fig. 8 shows simulation results of the analytical and FEA model, operated at no-load and $3000\,\mathrm{rpm}$. Fig. 9 shows simulation results of the analytical and FEA model, operated at nominal load and $3000\,\mathrm{rpm}$. Table IV summarizes the average torque $\overline{T}_\mathrm{el}$, the second harmonic of the torque $^2T_\mathrm{el}$ and the fundamental waves of the fault current $^1i_\mathrm{F1}$ and $^1i_\mathrm{F2}$ for $t \geq 15\,\mathrm{ms}$. Higher harmonics are not regarded for the comparison, because they are neglected in the analytical model. The average torque differs in case of two inter-turn faults by $6\,\%$ for the no-load operation and by $2\,\%$ for the nominal load operation. The second harmonic of the torque differs by approximately $9\,\%$ and the amplitude of the fault currents differs by approximately $5\,\%$ for both cases. The differences occur mainly because of the linearization at the nominal operating point. This explains, why there is an increased deviation of the average torque for the no-load operation. The machine behavior during the fault depends on the angular velocity, the phase currents and the fault network. This means the relative differences of the simulation results can be reduced by increasing the fault resistors, reducing the angular velocity and reducing the phase currents.
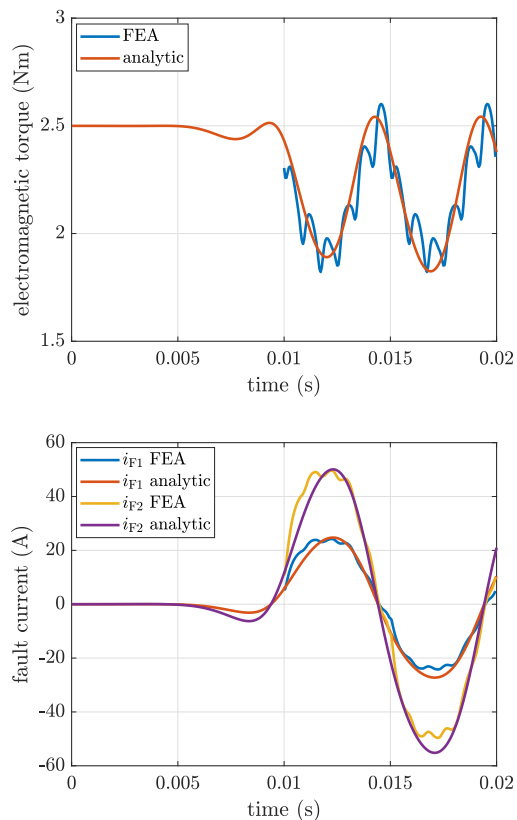
Fig. 9. Simulation results of the analyzed fault network in coil C1 of the stator winding. A current source with i_q = 8.4 A and i_d = -1.5 A is used for the power supply and the rotor speed is 3000 rpm.

VI. Conclusion and Future Work

The presented analytical model allows the simulation of PMSMs with stator winding faults on turn level. In contrast to existing models, this model is able to consider different inductance in the d- and q-axis. This means that the phase inductance can be dependent on the rotor position, which is the case for buried magnets. Furthermore, the model is able to analyze time-variant fault networks with any type of passive

TABLE IV
RESULTS

parameters	FEA	analytic
no-load operation		
$\overline{T}_{el}$	-0.152 Nm	-0.161 Nm
$^2T_{el}$	-0.145 Nm	-0.160 Nm
$^1i_{F1}$	13.2 A	13.9 A
$^1i_{F2}$	26.6 A	27.9 A
nominal load operation		
$\overline{T}_{el}$	-2.21 Nm	-2.16 Nm
$^2T_{el}$	0.30 Nm	0.33 Nm
$^1i_{F1}$	26.8 A	28 A
$^1i_{F2}$	53.1 A	56 A

components. This means the fault network is not limited to ohmic inter-turn faults. Phase-to-phase and phase-to-ground faults can be simulated and the fault network can include capacitors to account for high frequency currents caused by a frequency converter. In addition, the angular velocity is variable during the simulation, thus transient changes can be considered. The acausal implementation offers the advantage that different operating modes can be used for the simulation. Either a current source or a current controlled voltage source can be used for the power supply and it is possible to simulate the no-load behavior. There is a small difference of the simulation results compared to the FEA simulation mainly due to the neglected nonlinear magnetic circuit. In contrast, the computation time of the analytical model is about 200 times faster. Also, the FEA simulation does not offer time-variant resistor and a variable angular velocity.

We will use the presented model in our future work for a precise analysis of the machine behavior and the results of the analysis will allow a subsequent development of a reliable fault management system.

REFERENCES

[1] A. Mohammadpour, S. Mishra, and L. Parsa, "Fault-tolerant operation of multiphase permanent-magnet machines using iterative learning control," *IEEE Journal of Emerging and Selected Topics in Power Electronics*, vol. 2, no. 2, pp. 201–211, June 2014.

[2] R. Isermann, *Mechatronische Systeme: Grundlagen*. 2. Auflage, Springer-Verlag, ISBN 978-3-540-32336-5, 2007.

[3] Y. Lee and T. G. Habetler, "An on-line stator turn fault detection method for interior pm synchronous motor drives," in *APEC 07 - Twenty-Second Annual IEEE Applied Power Electronics Conference and Exposition*, Feb 2007, pp. 825–831.

[4] G. M. Joksimovic and J. Penman, "The detection of inter-turn short circuits in the stator windings of operating motors," *IEEE Transactions on Industrial Electronics*, vol. 47, no. 5, pp. 1078–1084, Oct 2000.

[5] J. Farooq, T. Raminosoa, A. Djerdir, and A. Miraoui, "Modelling and simulation of stator winding interturn faults in permanent magnet synchronous motors," *COMPEL -The international journal for computation and mathematics in electrical and electronic engineering*, vol. 27, no. 4, pp. 887–896, 2008.

[6] L. Romeral, J. Urresty, J. Ruiz, and A. Espinosa, "Modeling of surface mounted permanent magnet synchronous motors with stator winding interturn faults," *IEEE Transactions on Industrial Electronics*, vol. 58, no. 5, pp. 1576–1585, May 2011.

[7] J. Hang, J. Zhang, M. Cheng, and J. Huang, "Online interturn fault diagnosis of permanent magnet synchronous machine using zero-sequence components," *IEEE Transactions on Power Electronics*, vol. 30, no. 12, pp. 6731–6741, 2015.

[8] M. Kaufhold, H. Aninger, M. Berth, J. Speck, and M. Eberhardt, "Electrical stress and failure mechanism of the winding insulation in pwm-inverter-fed low-voltage induction motors," *IEEE Transactions on Industrial Electronics*, vol. 47, no. 2, pp. 396–402, 2000.

[9] J. R. Hendershot and T. J. E. Miller, *Design of brushless permanent-magnet machines*. Motor Design Books, 2010.

[10] O. A. Mohammed, S. Liu, and Z. Liu, "Physical modeling of pm synchronous motors for integrated coupling with machine drives," *IEEE Transactions on Magnetics*, vol. 41, no. 5, pp. 1628–1631, 2005.

[11] L. Quval and H. Ohsaki, "Nonlinear abc-model for electrical machines using n-d lookup tables," *IEEE Transactions on Energy Conversion*, vol. 30, no. 1, pp. 316–322, March 2015.

[12] C. Kral and D. Simic, "Simulation von Elektrofahrzeugen," *e & i Elektrotechnik und Informationstechnik*, vol. 128, no. 1, pp. 28–35, Feb 2011.